AMERICAN
METEOROLOGICAL
SOCIETY

Journal of Hydrometeorology

EARLY ONLINE RELEASE

This is a preliminary PDF of the author-produced manuscript that has been peer-reviewed and accepted for publication. Since it is being posted so soon after acceptance, it has not yet been copyedited, formatted, or processed by AMS Publications. This preliminary version of the manuscript may be downloaded, distributed, and cited, but please be aware that there will be visual differences and possibly some content differences between this version and the final published version.

The DOI for this manuscript is doi: 10.1175/JHM-D-11-016.1

The final published version of this manuscript will replace the preliminary version at the above DOI once it is available.

© 2011 American Meteorological Society

AMERICAN METEOROLOGICAL SOCIETY 1919

The 2010 Pakistan Flood and Russian Heat Wave:

Teleconnection of Hydrometeorologic Extremes

William K. M. Lau

Laboratory for Atmospheres, NASA Goddard Space Flight Center, Greenbelt MD, 20771

Kyu-Myong Kim*

Goddard Earth Sciences and Technology Center, U. of Maryland Baltimore County,

Baltimore Maryland, 21228

J. Hydrometeorology

Re-Revised July 2011

PRELIMINARY ACCEPTED VERSION

Corresponding author: William K. M. Lau, Laboratory for Atmospheres, NASA Goddard Space Flight Center, Greenbelt, MD 20771. Email: William.K.Lau@nasa.gov. Tel: 301-614-6332

*Current affiliation: GESTAR, Morgan State University, Baltimore Maryland, 21251

Abstract

In this paper, we present preliminary results showing that the two record setting extreme events during 2010 summer, *i.e*., the Russian heat wave/wild fires and Pakistan flood were physically connected. We find that the Russian heat wave was associated with the development of an extraordinary strong and prolonged extratropical atmospheric blocking event, and excitation of a large-scale atmospheric Rossby wavetrain spanning western Russia, Kazakhstan, and northwestern China/Tibetan Plateau region. The southward penetration of upper level vorticity perturbations in the leading trough of the Rossby wave was instrumental in triggering anomalously heavy rain events over northern Pakistan and vicinity in mid-to-late July. Also shown are evidences that the Russian heat wave was amplified by a positive feedback through changes in surface energy fluxes between the atmospheric blocking pattern and an underlying extensive land region with below- normal soil moisture. The Pakistan heavy rain events were amplified and sustained by strong anomalous southeasterly flow along the Himalayas foothills and abundant moisture transport from the Bay of Bengal in connection with the northward propagation of the monsoonal intraseasonal oscillation.

1. Introduction

During late July and early August 2010, Pakistan suffered a cluster of torrential rain event causing the worst flood in 100 years. According to the reports of the World Meteorological Organization (WMO 2011), 1700 people and 1.8 million homes perished and 20 million were rendered homeless, with an economic loss estimated to be more than 40 billion. At about the same time, western Russia was stricken by a record heat wave and a prolonged drought. Intense and extensive wild fires raged over more than 5000 km^2 of forested area over western Russia. The Russia heat wave and forest fires might have taken over 15,000 lives and cost the economy loss more than 15 billion. Both events represented profound humanitarian disasters that called for detailed scientific investigations. Already a number of studies on Pakistan flood (Houze et al. 2011, Webster et al., 2011 and Wang et al. 2011) and on the Russian heat wave (Schubert et al. 2011, Matsueda 2011, and Dole et al. 2011) are now emerging. However these studies were focused mostly on the details of each individual event separately. In this study, we focus on the teleconnection and feedback mechanisms underlying the Russian heat wave and the Pakistan flood. As such, our paper seeks to provide a new and complementary perspective to the aforementioned studies.

2. Data

For this study, we used a combination of in-situ, satellite and reanalysis data to carry out correlative and diagnostic analyses. For rainfall, we used daily gridded rain gauge data from NOAA Climate Prediction Center (CPC) (Xie et al. 2007), as well as daily rainfall product (3B42) on 0.25 x 0.25 degree latitude-longitude grid from the Tropical Rainfall Measuring Mission

(TRMM) (Huffman et al. 2007). Surface temperature was obtained from the Advanced Infra Red Sounder (AIRS), and fire counts and cloudiness data were from the Moderate Resolution Imaging Spectro-radiometer (MODIS) on board the NASA Aqua and Terra satellites. AIRS is a high spectral resolution spectrometer on board Aqua satellite with 2378 bands in the thermal infrared (3.7 - 15.4 μm) and 4 bands in the visible (0.4 - 1.0 μm). The MODIS Fire Pixel Count has a spatial resolution of 1kmx1km and is determined by a significant increase in radiance at 4um compared to 11um radiance. It is available from the Terra and Aqua satellites twice daily, night and day. Data and meta-data for AIRS and MODIS fire pixel data were available from at the Goddard Earth Sciences Data and Information Service Center (GES DISC, http:// disc.sci.gsfc.nasa.gov/) and MODIS Hotspots/Active Fires Text file FTP site (ftp://mapsftp.geog.umd.edu), respectively. For geopotential height, wind, and moisture, we used assimilated data from the NASA Modern Era Retrospective-analysis for Research and Applications (MERRA, Rienecker et al. 2011) available from the Goddard Modeling and Assimilation Office and the GES DISC.

3. Background

a) Pakistan flood

Located in the northwestern corner of the Indian subcontinent, Pakistan is a relative dry region. Even during the peak of the monsoon season, July-August, the average total rainfall over the wettest part of the country (northern Pakistan) is of the order of 160-180 mm – a scanty amount compared to rain total of 1600-2000 mm for the same months over northeastern India and the Bay of Bengal. During July-August 2010, rainfall over northern

Pakistan occurred first episodically, with clusters of heavy rain events in July 11-12, and July 19-22 (Fig. 1a, bar graph). The most intense heavy rain occurred in July 27-29, followed immediately by a period of steady moderate-to-heavy rain up to the end of August. Widespread flooding over the Indus River Valley occurred soon after the heavy rain of July 27-29. We note that while there may be systematic bias in the actual magnitude of the TRMM rainfall over land compared with others, all data show temporal consistency in the occurrence of episodic rain events over northern Pakistan (cf. Webster et al. 2011). Here, we stress that the flooding was unlikely the result of just any singular major heavy rain event, but rather the cumulative effects of all the episodic heavy rain events in July, causing increased storm water run-off and saturation of soil moisture, and escalated further by the steady rain in August. The heavy rain events in July-August, plunged approximately one-fifth of the country underwater (Dartmouth Flood Observatory Archives, http://www.dartmouth.edu /~floods/Current.htm). As shown in Fig. 1a, the magnitude of the heavy rain events in 2010 far exceeded the 2-σ deviation based on the 12 years (1998-2009) of TRMM rainfall data. During the 2 week period, July 25- August 8, 2010, CPC rainfall data showed that heavy rain of approximately 500 mm fell in about 10 days in the northern Pakistan Swat Valley, approximately 300% of the climatological rainfall total over the same region in July and August . As evident in the rainfall anomaly pattern shown in Fig. 1b, the heavy rain over northern Pakistan was not isolated geographically, but appeared to be associated with a northeastward shift of the entire South Asia monsoon system, featuring excessive monsoon rainfall over northeastern India along the foothills of the Himalaya, northeastern India and Bangladesh, and

northeastern Arabian Sea, coupled to reduced rainfall over central and southern India and the Bay of Bengal.

b. Russian heat wave

Summertime atmospheric blocking associated with heat wave, drought and wild fires occurs commonly over northern Eurasia (Groisman et al. 2007, Girardin et al. 2009). In July-August 2010, a record heat wave developed and prevailed over western Russia. AIRS data shows that the surface temperature (upper curve, Fig. 1a) over western Russia rose rapidly around June 20, remained at a high level for the next 10 days, and intensified from around July 18, with maximum area-averaged temperature exceeding nearly 8-10^{o} C above the seasonal mean (2003-2009). On August 18, a cold front passed through and brought rain to western Russian, terminating the heat wave. During the two-week period from July 25- August 8, coinciding with the maximum Pakistan rain, the heat wave expanded to Eastern Europe and western Siberia, as shown by the area of positive surface temperature anomaly, surrounded by pronounced negative temperature anomalies especially over western Siberia (Fig. 1c). The extreme hot and dry weather spurred ferocious forest fires over the vast taiga regions of western Russia and the Ukraine, as evident in the density of the satellite observed MODIS fire pixels shown in Fig. 1c. Fig. 2 shows the blocking index, as defined by the number of blocked days in the latitude belt 40-80^{o} N during the summer (JJA) as a function of longitude. At each longitude, a block is identified when the 5-day mean 500 hPa meridional height gradients exceed given thresholds (Tibaldi and Molteni 1990). Based on this index, the 2010 blocking event was unusual in that a) its magnitude was more than three-times the mean blocking index, exceeding by far the 2σ level of the climatological variability, b) it was shifted about 10^{o}

longitude east of the climatological position near 25-30^{o} E, and c) it covered a longitudinal span 20 – 70^{o} E, much larger than the climatology .

4. Teleconnection

To facilitate the discussion of teleconnectivity, evolution, and feedback mechanisms of the Russian heat wave and Pakistan flood, we next describe the quasi-stationary atmospheric patterns during two consecutive 15-day periods, July 10- 24, and July 25- August 8, before and during the transition from the episodic to the steady rain regimes over northern Pakistan, respectively.

a. Period I: July 10- July 24

This period characterized the development of the Russian heat wave in conjunction with the episodic rainfall events over northern Pakistan. A 500 hPa blocking high over western Russia was found, with a leading trough to its east, spanning western Siberia and regions north of Iran and Pakistan (Fig. 3a). The blocking was associated with a splitting of the 200hPa jet stream into a northern branch over the polar region [60 -70^{o} N, 10- 60^{o} E], and a more-or-less continuous subtropical branch near 40^{o} N across the domain. As a point for later reference, the 5850 m geopotential height (thick solid line in Fig. 3a), which meandered between 40 -30^{o} N, appeared to separate the extratropics from the tropics. The blocking high and associated wave structure in the mid-troposphere, and accompanying circulation moisture fields in the lower troposphere were very pronounced as shown in the anomaly fields in Fig. 4a and b. At 500 hPa, the blocking high over western Russia was coupled to a bow-shaped deep trough, with two pronounced low pressure centers (labeled L in Fig. 4a) to its east, and another high

pressure feature further east over central Siberia. The southern portion of the trough displayed a pronounced southwest-to-northeast tilt, penetrating into the subtropics with a well-defined low center located north of Pakistan. The wave pattern resembled that of a dispersive Rossby wave-train (Hoskins and Ambrizzi, 1993) emanating from the blocking high over western Russia, and propagating towards the northeast and southeast directions. Matsueda (2011) and Schubert et al (2011) also noted similar Rossby wave features associated with the 2010 Russian heat wave.

Coupled to the 500 hPa blocking high was a lower troposphere large-scale anticyclone (Fig. 4b). The equatorward flow on the eastern side of the anticyclone brought widespread cooler and drier (sinking) air over western Siberia to regions further south, over Kazakhstan and Iran. Over the mountainous region of Afghanistan and Pakistan, the low-level flow was not well organized. However, over the South Asian monsoon region, two distinct branches of anomalous low- level flow could be identified. An anomalous low-level easterly flow from the Bay of Bengal was found over central and northern India, implying an anomalous transport of moisture from the Bay of Bengal to northwestern India. Additionally, an anomalous southerly low-level flow was found over northern Arabian Sea. Analysis (figure omitted) showed that the northern Arabian Sea was warmer than normal, in conjunction with the occurrence of La Nina in the tropical Pacific during the summer of 2010. The warmer Arabian Sea could increase evaporation, allowing more moisture transport by the anomalous southerlies into the Gulf of Oman and southern coast of Pakistan (Fig. 4b).

b. Period II: July 25 – Aug 8

During this period, the heat wave intensified and the Russian wild fires grew in area coverage and intensity. At 500 hPa, the quasi-stationary blocking high shifted about 10^{o} eastward in longitude and grew to a very impressive size and magnitude with a characteristic Ω–block anticyclonic pattern that split the 200hPa jet stream into a distinct polar, and a subtropical branch respectively (Fig. 3b). The subtropical branch developed a "kink" west of northern Pakistan with strong jet acceleration downstream of the mid- tropospheric trough which penetrating from the extratropics to tropics. The pattern of the 5850 m geopotential contour (thick solid line in Fig. 3b) implies strong geostrophic flow associated with the blocking high from near 60^{o} N to the subtropics below 30^{o}N (Fig. 3b). The anomaly fields (Fig. 4c) shows that the 500 hPa anticyclone shifted eastward over western Russia. The trough at the leading edge of the anticyclone separated distinctly into an extratropical and a tropical component. The tropical component was characterized by, a well-defined mid-tropospheric subtropical low with a closed cyclonic circulation (labeled C_1 in Fig. 4c) near 25-35^{o} N, immediately west of northern Pakistan. As discussed previously, the monsoon rain system had shifted northeastward by this time. Indeed, C_1 appeared to be only a part of a large-scale anomalous circulation pattern of the entire South Asian monsoon system, which included the development of a secondary closed cyclonic circulation (marked C_2 in Fig. 4c) over southern Pakistan and northeastern Arabian Sea, and an anomalous anticyclonic circulation over western China, northeast of the Tibetan Plateau. The tight pressure gradient between the Tibetan High and the cyclonic low system (C_1-C_2) forced strong mid-tropospheric southeasterlies over northern India and southerlies over northern Pakistan, bringing additional moisture from the Bay of Bengal and the northern Arabian Sea. The anomalous mid-

tropospheric low and high pressure system over the Tibetan Plateau was also noted by Houze et al. (2011) as a part of the very unusual circulation pattern associated with the 2010 Pakistan flood. The quasi-stationary monsoon cyclonic features were similar to those of hybrid mid-latitude and tropical weather system, called Mid-Tropospheric Cyclones (MTC) over the subtropical Asian monsoon region (Mak 1975, Carr 1977, Goswami et al. 1980). The MTCs are well-known rain-bearing systems with a warm core above, and cold core below 600 hPa, upper level divergence, mid-tropospheric cyclonic flow and ascent, but generally weak organization near the surface (Krishnamurti and Hawkins 1970).

During Period-II, in conjunction with the development of the 500 hPa blocking pattern, the low level anticyclone over northern Europe and Russia also shifted eastward to western Siberia (Fig. 4d). On the southeastern side of the anticyclone, the low level northeasterly, and northerly flow brought a tongue of dry and cold (sinking) air from Siberia to Iran and eastern Pakistan, setting the stage for a confrontation with the warm, moist (rising) air transported northwestward from Bay of Bengal, creating large temperature and moisture contrast favorable for monsoon cyclone development over northern Pakistan. The upper level disturbances embedded in the leading trough of the Rossby wave were associated with strong upper level cyclonic vorticity, wind divergence, and 500 hPa ascent (see also Fig. 5) east of the mid-tropospheric low center. These mid- and upper tropospheric forcing would act like a pump drawing the low level southeasterly flow over northern India, along the Indian/Nepal Himalayas, thereby transporting additional moisture from the Bay of Bengal to Pakistan (Fig. 4d). The moist southeasterly flow along the Himalayas foothills was also strengthened by the development of a monsoon trough (thick blue solid line in Fig. 4d) associated with the

northward propagation of monsoon intraseasonal oscillations (see further discussion in Section 6).

5. Triggering and local feedback processes

To illustrate the extratropical triggering of the Pakistan rain events, Figure 5 shows the 4-day (July 26-29) evolution of 300 hPa relative vorticity, 500 hPa height and vertical motions, and TRMM rainfall leading up to and during the maximum rain event (July 27-29) over northern Pakistan. The quasi-stationary blocking anticyclone (Fig. 5, left panels) with associated large-scale mid-tropospheric subsidence (regions shaded blue in Fig. 5, middle panels) over western Russia can be seen in all four days. On July 26, a day before the occurrence of heavy rain over northern Pakistan, an upper-level V-shaped positive (cyclonic) vorticity filament was formed at the southeastern edge of the 500 hPa anticyclone, dipping into the target region (marked by rectangle in Fig. 5). This vorticity feature moved southward and eastward through the target region in the next three days (Fig. 5, left panels). It penetrated furthermost into the subtropics near 30-35^{o} N during July 27-29. Strong rising motion was found immediately to the east of the vorticity anomalies (Fig. 5, middle panels) coinciding with the peak rainfall in northern Pakistan (Fig. 5, right panels). Note that on July 26, the rainfall maximum was still concentrated over the Bay of Bengal, the Himalaya foothills and northeastern Arabia Sea. By July 28-29, the maximum rainfall has shifted to over northern Pakistan. Similar sequences of events indicating extratropical triggering were found for the subsequent cluster of heavy rain events centered around August 3, and August 6 in Period II, as well as July, 12 and July 20 in Period I. For more details on the daily variations of surface temperature, upper troposphere circulation over

Eurasian, rainfall variations over Pakistan and India for the period July 1 through August 15, an online movie and narrative are available in Lau and Kim (2011, http://www.earthzine.org/2011/06/01/did-the-russian-heat-wave-trigger-the-pakistan-heavy-rain-in-2010/)

Next, we present evidence of plausible local feedback mechanisms for the two extreme events and their connections. For the Russian drought, the positive feedback was likely to occur in association with the below-normal soil moisture indicated by MERRA (not shown) over West Russian at the start of the blocking in early June. As the blocking event commenced around mid-June (see Fig. 1a), the associated subsidence caused adiabatic atmospheric warming and drying by entrainment of dry air from above. The warmer and drier air suppressed rain and clouds, and accentuated the initial drying of the land. During Period-I (Fig. 6a), accompanying the land drying there was a substantial reduction in cloudiness, up to 20% over the blocking region of western Russian and northeastern Europe (Fig. 6a). The reduced clouds increased downward surface solar radiation with mean anomaly magnitude ~20 Wm^{-2} over the blocking region (Fig. 6b), enhancing surface warming there. The reduced soil moisture led to a reduction in evaporation (~ -10 Wm^{-2}) latent heat flux from land to atmosphere. The initial drier land, the increased surface shortwave radiation and the reduced evaporation all conspired to the rapid warming of the surface air and land (see also Fig. 1a). The large increase in sensible heat flux (~+15 Wm^{-2}) and longwave radiation flux (~ +10 Wm^{-2}) reflected the increasing land surface temperature as the land surface equilibrated energetically. During Period-II, the surface shortwave continued to increase as more clouds were depleted over an even larger areas (Fig. 6c), as the heat wave and the blocking high deepened and shifted westward. The increase in cloudiness associated with heavy rain over northern Pakistan

and vicinity is also clearly seen in Fig. 6c. All anomalous surface fluxes remained unchanged in sign compared to Period-I, but were substantially (~25%) amplified (Fig. 6d) . Further reduction in clouds and precipitation (due to lack of surface evaporation) allowed more downward solar radiation, resulting in more warming and desiccation of the land, causing even more reduction in cloud and precipitation and increase in atmospheric stability. Thus the blocking anticyclone was intensified and prolonged, enabling deeper tropical penetration of the upper level trough, and increased transport of cold dry Siberian low level air masses over the Pakistan region. Ferranti and Viterbo (2006) reported similar land-surface feedbacks in amplifying the 2003 summertime heat wave over Europe.

Moisture transport integrated between the surface and 850 hPa (Fig. 7a) indicates that during Period-I northern Pakistan and the foothill regions were still relatively dry compared to regions to the south. The moist monsoon westerly moisture transport was strongest across the Western Ghat of the Indian subcontinent near 15^{o} N. During this period, the Swat Valley region near 70-75^{o} E in northern Pakistan developed an above-normal moist environment locally (Fig.7b) mainly due to moisture transported from the Arabian Sea, increasing the moist instability, and potential convectivity in the region. However, the synoptic scale forcing with respect to moisture and temperature was not well organized. The deep layer of anomalous cold air over northern Pakistan would inhibit the development of organized deep convection, while the warmer air to the west appeared to be decoupled from the moisture field. In contrast, during Period-II , a pronounced tongue of strong northwestward moisture transport brought additional moisture from the Bay of Bengal along the Himalayas foothills to northern Pakistan (Fig. 7c). Here, the synoptic scale forcing become more organized, with the sinking

cold air to the west undercutting and lifting the warm air over northern Pakistan, creating a westward tilt with height (Fig. 7d). The elevated warmer air above 600 hPa over northern Pakistan provided the large-scale structure favorable for the development of warm core MTC's over the Asian monsoon region (Krishnamurti and Hawkins, 1970). Over northern Pakistan [65 -70^{o} E], strong ascending motion east of the 500 hPa low was found (see also Fig. 5 middle panels), consistent with the increased moisture supply, and frequent occurrence of heavy and steady rain spells over the region during Period-II. As discussed previously, the source of the low-level cold, dry sinking air was from western Siberia conveyed by the low-level anticyclonic flow from the Russian blocking high, while warm moist air was transported from low- level anomalous southeasterlies from the Bay of Bengal. The warming of the middle and upper troposphere by latent heat release and updrafts from heavy rains of the mid-tropospheric monsoon cyclones further enhanced low-level moisture from the Bay of Bengal, providing a positive feedback to the developing monsoon cyclones over the region.

6. Role of Monsoon Intraseasonal Oscillation (MISO)

Figure 8a shows the time-latitude cross section of TRMM daily rainfall and the associated monsoon low-level flow across the Pakistan-central India sector [70-80^{o} E] associated with the MISO during 2010 summer. The Indian monsoon onset occurred at around 14-15 June as signaled by the sudden appearance of strong steady low level westerlies and the MISO rainfall reaching 20^{o} N. Subsequently, successive northward surges of MISO rain clusters can be seen reaching the northernmost latitude near the Himalaya foothills [30-35^{o} N] near the end of July, from whence the rainfall became quite steady until the end of August. At the latitude 30-35

N, episodic rain events labeled by #1-5 can be identified with rainfall maxima shown in Fig. 1a. Events #1-3 were well separated from the main MISO. At the time of occurrence of event #4 (July 19-20) and #5 (July 27-29), there was a strong turning of the low level winds at 25-35^{o} N to southeasterlies and easterlies. This was associated with the development of the monsoon trough noted previous in Fig. 4d. At around the end of July to mid August, the prevailing easterly low-level winds at 25 -35^{o} N were found the latitudes of northern Indo-Gangetic Plain and the Himalaya foothills. The easterlies were associated with the westward moving cyclones along the Himalaya foothills (Houze et al. 2011). It appeared that during the early period of July, while central India and Pakistan were increasingly moistened by the seasonal monsoonal flow, abundant water vapor from the MISO had not yet reached the region. This is in agreement with recent finding of Wang et al. (2011) that rainfall events over northern Pakistan during July 2010 were episodic, stemming from local instability and possible triggering by upper level disturbances. Toward late July and August, as the MISO trough reached northern India and Pakistan, the prevailing low-level southeasterlies transported abundant moisture from the Bay of Bengal to the Himalayas foothills and northern Pakistan. This phase corresponds to the steady monsoon rain discussed earlier. The 2010 Pakistan MISOs were unusual compared to other years, in that the associated moisture surges reached far northward and stayed longer in the northern Indian Himalayas foothills region, and that were associated with strong low level southeasteries in northern India and Pakistan (30-35^{o} N). Examination of other years of TRMM rainfall data indicated that typically, the MISO rainfall and low level southeasterly wind signals along the Himalaya foothills were weak or absent. For comparison, the time cross-section for summer 1998 (Fig. 8b) which was also a transition year from El Nino

to La Nina shows that , in the latitude belt of northern India and northern Pakistan 30-35^{o} N, the MISO signals were weak, and only episodic rainfall occurred. This suggests that contemporaneous La Nina condition alone may not be sufficient to cause heavy rain events responsible for the 2010 Pakistan flood. Rather, the extreme northward excursion of the MISO may also play a key role. The abnormal conditions associated with the MISOs are also in agreement with Houze et al (2011) who found that cloud and rain systems normally associated with monsoon depression over the Bay of Bengal was shifted to northern Pakistan during 2010. At the final revision of this paper, we were brought to the attention of the work by Hong *et al* (2011) which showed observational evidences indicating the role of Rossby wave and monsoon surges in triggering the 2010 Pakistan heavy rain, consistent with our results. Even though these authors did not address the feedback mechanisms underlying the intensity and prolonged Russian heat wave and the Pakistan heavy rain, their results further strengthen the notion that the two extreme events are physically connected.

7. Conclusions

We presented preliminary evidence suggesting that the two extreme events in the summer of 2010*, i.e.,* the Russia heat wave and the Pakistan flood were meteorologically connected. Both events were unusual in that the magnitudes of the anomalies far exceeded by more than 2-σ their respective climatological variability. The Russian heat wave was unusual in size and magnitude and its eastward location compared to climatology , and in the development of a pronounced blocking high with a well defined Ω-flow pattern, a split upper level jet stream, and deep trough penetrating to the subtropics over northern Pakistan. The

Pakistan heavy rain during late July and August was also coincident with the arrival of the northward propagation of the monsoon intraseasonal oscillation, coupled with increased southeasterlies moisture transport along the Himalayas foothills from the Bay of Bengal to northern Pakistan.

Based on the above results, we argued that the intense and prolonged atmospheric blocking situation, associated with the extreme heat wave over western Russia was instrumental in forcing a large-scale atmospheric Rossby wave train connecting western Russia and the South Asian subtropical monsoon region. Upper level vorticity perturbations in the leading trough of the Rossby wave train penetrating from the extratropics to the subtropics triggered upward motion ahead (east) of the perturbations, leading to the development of mid-tropospheric cyclonic anomalies west of northern Pakistan, with cold core below and warm core above 600 hPa. Our analysis also showed that unusual conditions in the South Asian monsoon region may also play an important role in enhancing the Rossby wave forcing by amplifying and sustaining the Pakistan rainfall events via increased moisture transport from the Bay of Bengal associated with the extreme northward reach of monsoon intraseasonal oscillations over northern India and Pakistan in late July to August 2010. Well designed numerical experiments are needed to test the proposed hypothesis, and to tease out the relative importance of extratropical vs. tropical forcing in leading to the 2010 Pakistan heavy rain events.

Acknowledgements

This work was supported by the NASA Interdisciplinary Investigation, and the Tropical Rainfall Measuring Mission (TRMM). K-M Kim was supported by the Korean Meteorological Administration Research and Development Program under Grant RACS_2010-2018. We thank two anonymous reviewers for their critical and detailed review of the paper.

References

Carr, F. H., 1977: Mid-tropospheric cyclones of the summer monsoon. *Pure Appl. Geophys*. **115**, 1383-1412.

Dole, R., M. Hoerling, J. Perlwitz, J. Eischeid, P. Pegion, T. Zhang, X-W Quan, T. Xu, and D. Murray, 2011: Was there a basis for anticipating the 2010 Russian heat wave? *Geophys. Res. Lett*., **38**, L06702, doi:10.1029/2010GL046582.

Ferranti, L., and P. Viterbo, 2006: The European Summer of 2003: Sensitivity to Soil Water Initial Conditions. *J. Climate* **19**, 3659–3680.

Girardin, M. P., A. A. Ali, C. Carcaillet, M. Mudelsee, I. Drobyshev, C. Hely, Y. Bergeron, 2009: Heterogeneous response of circumboreal wildfire risk to climate change since the early 1900s. *Global Change Biology* **15**, 2751–2769, doi: 10.1111/j.1365-2486.2009.01869.x.

Goswami, B. N., R. N. Keshavamurty, and V. Satyan, 1980: Role of barotropic, baroclinic and combined barotropic-baroclinic instability for the growth of monsoon depressions and mid-tropospheric cyclones. *J. Earth Sys. Sci.* **89**, 79-97.

Groisman, P.Y., B. G. Sherstyukov, , V. N. Razuvaev, R. W. Knight, J. G. Enloe, N. S. Stroumentova, P. H. Whitfield, E. Forland, I. Hannsen-Bauer, H. Toumenvirta, H. Aleksandersson, A. V. Mescherskaya, and T. R. Karl, 2007: Potential forest fire danger over Northern Eurasia: changes during the 20th century. *Global and Planetary Change* **56**,371–386 .

Hong, C. C. H. H. Hsu, N. H. Lin and H. Chiu, 2011: Roles of European blocking and tropical-extratropical interaction in the 2010 Pakistan flooding. *Geophy. Res. Lett.*, **38**, L13806, doi:10.1029/2011GL047583.

Hoskins, B. J. and T. Ambrizzi, 1993: Rossby Wave Propagation on a Realistic Longitudinally Varying Flow. *J. Atmos. Sci.* **50**, 1661-1671.

Houze, J.A., K. L. Rasmussen, S. Medina, S. R. Brodzik, and U. Romatschke, 2011: Anomalous atmospheric events leading to the 2010 floods in Pakistan. *Bull. Amer. Meteor. Soc*., **92**, 291–298. doi: 10.1175/2010BAMS3173.1

Huffman, G. J., R. F. Adler, D. T. Bolvin, G. Gu, E. J. Nelkin, K. P. Bowman, Y. Hong, E. F. Stocker, and D. B. Wolff, 2007: The TRMM Multisatellite Precipitation Analysis (TMPA): Quasi-Global, Multiyear, Combined-Sensor Precipitation Estimates at Fine Scales. *J. Hydrometeor.* **8**, 38–55.

Krishnamurti, T. N., and R. S. Hwakins, 1970: Mid-Tropospheric Cyclones of the Southwest Monsoon. *J. Appl. Meteor*. **9**, 442-458.

Lau, K. M. , and K. M. Kim, 2011: Did the Russian heat wave trigger the Pakistan flood in 2010? *Earthzine*, http://www.earthzine.org/2011/06/01/did-the-russian-heat-wave-trigger-the-pakistan-heavy-rain-in-2010/.

Mak, M. K., 1975:The Monsoonal Mid-Tropospheric Cyclogenesis. *J. Atmos. Sci.* **32**, 2246-2253 .

Matsueda, M., 2011: Predictability of Euro-Russian blocking in summer of 2010. *Geophy. Res. Lett*., **38**, L06801, doi:10.1029/2010GL046557.Rienecker, M. M., and coauthors, 2011: MERRA - NASA's Modern-Era Retrospective Analysis for Research and Applications. J. Climate, doi: 10.1175/JCLI-D-11-00015.1 (in press)

Rienecker M. M., M. J. Suarez, R. Gelaro, R. Todling, J. Bacmeister, E. Liu, M. G. Bosilovich, S. D. Schubert, L. Takacs, G.-K. Kim, S. Bloom, J. Chen, D. Collins, A. Conaty, A. da Silva, W. Gu, J. Joiner, R. D. Koster, R. Lucchesi, A. Molod, T. Owens, S. Pawson, P. Pegion, C. R. Redder, R.

Reichle, F. R. Robertson, A. G. Ruddick, M. Sienkiewicz, J. Woollen, 2011: MERRA—NASA's Modern-Era Retrospective Analysis for Research and Applications. *J. Climate*, DOI: 10.1175/JCLI-D-11-00015.1.

Schubert, S., H. Wang and M. Suarez, 2011: Warm season subseasonal variability and climate extremes in the northern Hemisphere: The role of stationary Rossby waves. *J. Climate* (submitted).

Tibaldi, S. and F. Molteni, 1990: On the operational predictability of blocking. *Tellus*, **42A**, 343-365.

Wang S. Y., R. E. Davis, W. R. Huang, and R. R. Gilllies, 2011: Pakistan's two-stage monsoon and links with the recent climate change. *J. Geophys. Res*., (submitted).

Webster, P. J., V. E. Toma, and H.-M. Kim, 2011: Were the 2010 Pakistan floods predictable?, *Geophys. Res. Lett*., **38**, L04806, doi:10.1029/2010GL046346.

WMO, 2011: Weather extremes in a changing climate. Hindsight on foresight. WMO-No. 1075, 17pp.

Xie, P., M. Chen, S. Yang, A. Yatagai, T. Hayasaka, and Y. Fukushima, 2007: A gauge-based analysis of daily precipitation over East Asia, *J. Hydrometeor*., **8,** 607-626.

Figure Captions

Figure 1 a) Time series of AIRS daily surface temperature (^{o}C) averaged over western Russia [45-65^{o} N, 30-60^{o}E], with positive (negative) deviations from climatology shaded red (blue), and TRMM daily rainfall (mm day^{-1}, left ordinate) over northern Pakistan [32-35^{o}N, 70-73^{o}E], for the June 1 - August 27, 2010. Spatial distribution of b) TRMM rainfall anomaly over Pakistan and the South Asian monsoon region for period July 25 – Aug 8, 2010, c) AIRS surface temperature anomaly, and MODIS daily fire pixel (green dots) for the same period. The rainfall anomaly (mm day^{-1}) was derived from the base period of 1988-2009, and the surface temperature anomaly (^{o}C) from the base period of 2003-2009.

Figure 2 Number of blocking events at each longitude during boreal summer (JJA) for 2010 (blue) and climatological mean distribution of atmospheric blocking from 1979-2009. Yellow and Orange layers indicating one and two standard deviation from mean respectively. Blue dots indicate longitudinal locations where the blocks in 2010 were at all time high since 1979.

Figure 3 Spatial patterns of 500 hPa geopotential height (contour) and 200hPa wind speeds during a) Period I and b) Period II.

Figure 4 Spatial patterns of a) 500 hPa geopotential height (in m) and wind anomalies during Period-I, b) 850 hPa wind and precipitable water (in mm) below 500hPa during Period-I, c) 500 hPa geopotential height and wind anomalies (ms^{-1}) during Period-II, and d) anomalous 850 hPa wind and precipitable water during Period-II. Centers of the

blocking high (H), and low (L) and the mid-tropospheric cyclones (C_1 and C_2) are marked. Thick line in Fig. 4d indicates the location of monsoon front. Anomalies were computed based on the climatology of 1979–2009.

Figure 5 Daily sequence during July 26-29 of MERRA 300 hPa vorticity (10^{-5} s^{-1}) and 500 hPa height (m)anomalies (left panels), 500 hPa vertical motion (Pa s^{-1}) (middle panels), and TRMM rainfall (right panels). The target region of northern Pakistan and vicinity to the west is indicated by the rectangle. The sign of the vertical motion (middle panels) is reversed so that positive value (red) indicates ascending motion.

Figure 6. Upper panels: Distribution of MODIS cloud fraction anomalies for a) Period I, and c) Period II. Anomalies were computed based on the climatology of March 2000-February 2010. Lower panels: Area mean MERRA shortwave (SW) and longwave (LW) radiation, latent heat (LH) and sensible heat (SH) flux, net flux (Net) at the surface, and soil moisture (SM) averaged over western Russia [45-65^{o} N, 30-60^{o}E] for b) Period I, and d) Period II. Units are W/m^2 for fluxes and fraction (times 100) for soil moisture. Red (blue) color denotes warming (cooling) of the land surface

Figure 7 Upper panels: Distribution of vertically integrated moisture transport between surface to 850hPa for a) Period I, and c) Period II. Amplitude is shown in shading. Lower panels: Composite longitude-height cross-section of temperature (shading) and moisture (contour) anomalies averaged between 32 N – 35N, during rainy days (rain rate > 1 mm day^{-1}) in the northern Pakistan (See Fig. 1) for b) Period I, and d) Period II.

Figure 8 Latitude-time cross section of TRMM daily rainfall (mm day^{-1}) and MERRA winds at 850hPa averaged between 70^{o}E and 80^{o}E for (a) 2010 and (b) 1998.

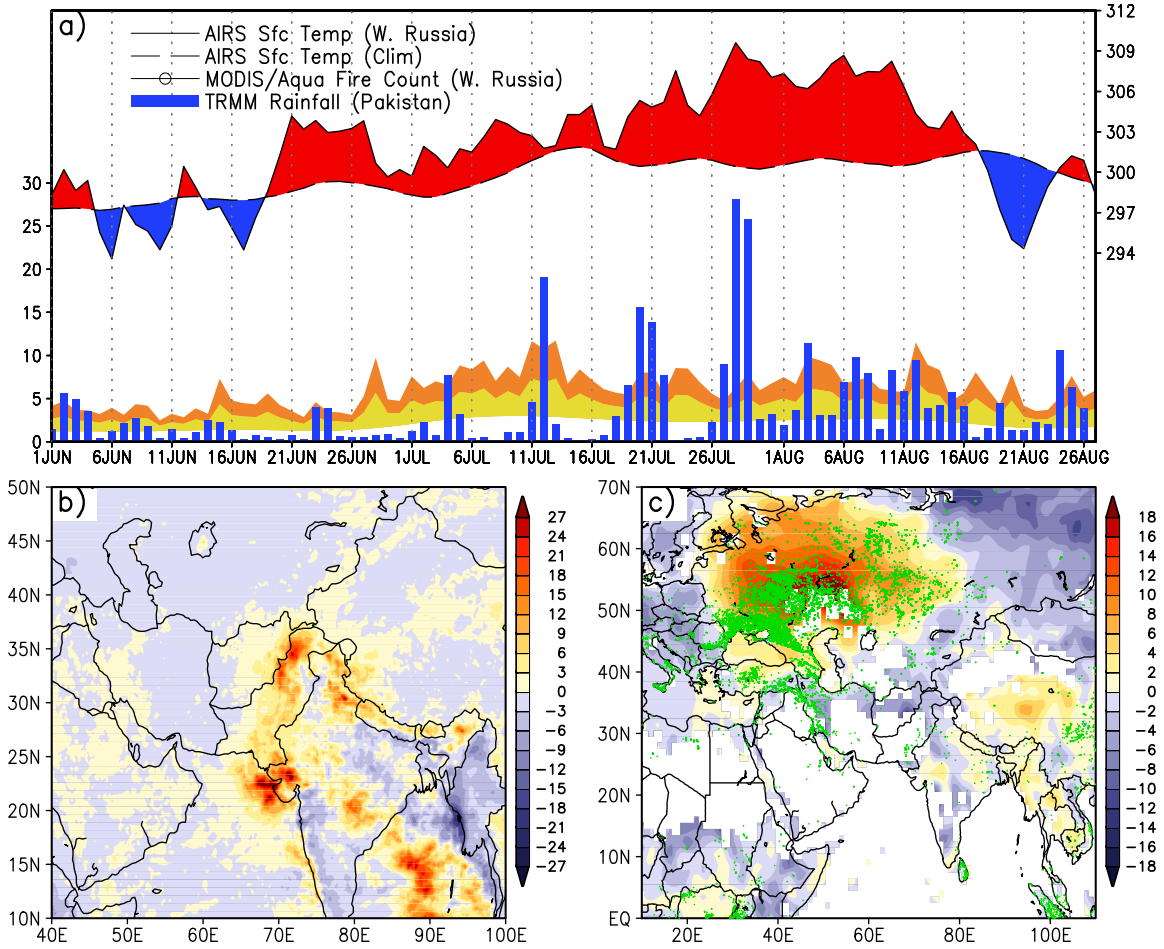

Figure 1 a) Time series of AIRS daily surface temperature (^{o}C) averaged over western Russia [45-65^{o} N, 30-60^{o}E], with positive (negative) deviations from climatology shaded red (blue), and TRMM daily rainfall (mm day^{-1}, left ordinate) over northern Pakistan [32-35^{o}N, 70-73^{o}E], for the June 1 - August 27, 2010. Spatial distribution of b) TRMM rainfall anomaly over Pakistan and the South Asian monsoon region for period July 25 – Aug 8, 2010, c) AIRS surface temperature anomaly, and MODIS daily fire pixel (green dots) for the same period. The rainfall anomaly (mm day^{-1}) was derived from the base period of 1988-2009, and the surface temperature anomaly (^{o}C) from the base period of 2003-2009.

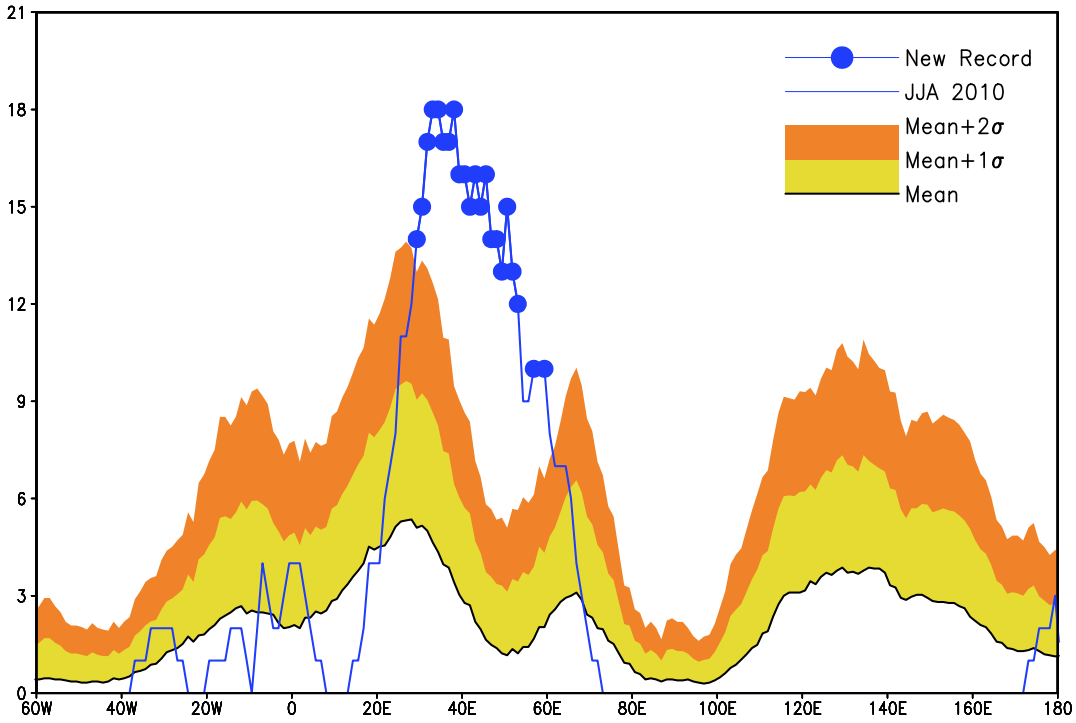

Figure 2 Number of blocking events at each longitude during boreal summer (JJA) for 2010 (blue) and climatological mean distribution of atmospheric blocking from 1979-2009. Yellow and Orange layers indicating one and two standard deviation from mean resepctively. Blue dots indicate the longitudinal locations where the occurrence of blocks in 2010 were at all time high since 1979.

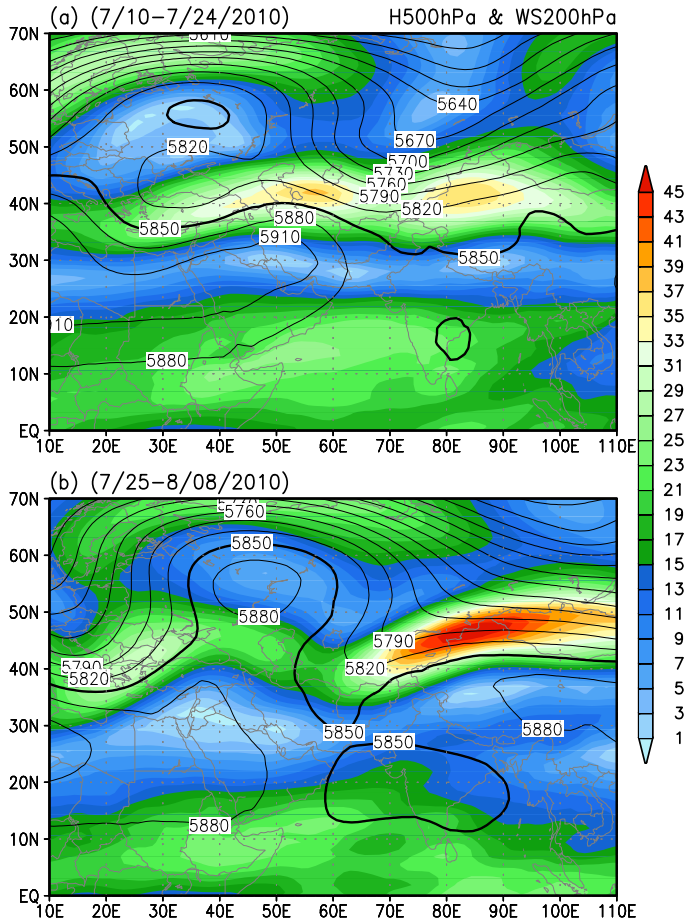

Figure 3 Spatial patterns of 500 hPa geopotential height (contour in m) and 200hPa wind speeds (in ms^{-1}) during a) Period I and b) Period II.

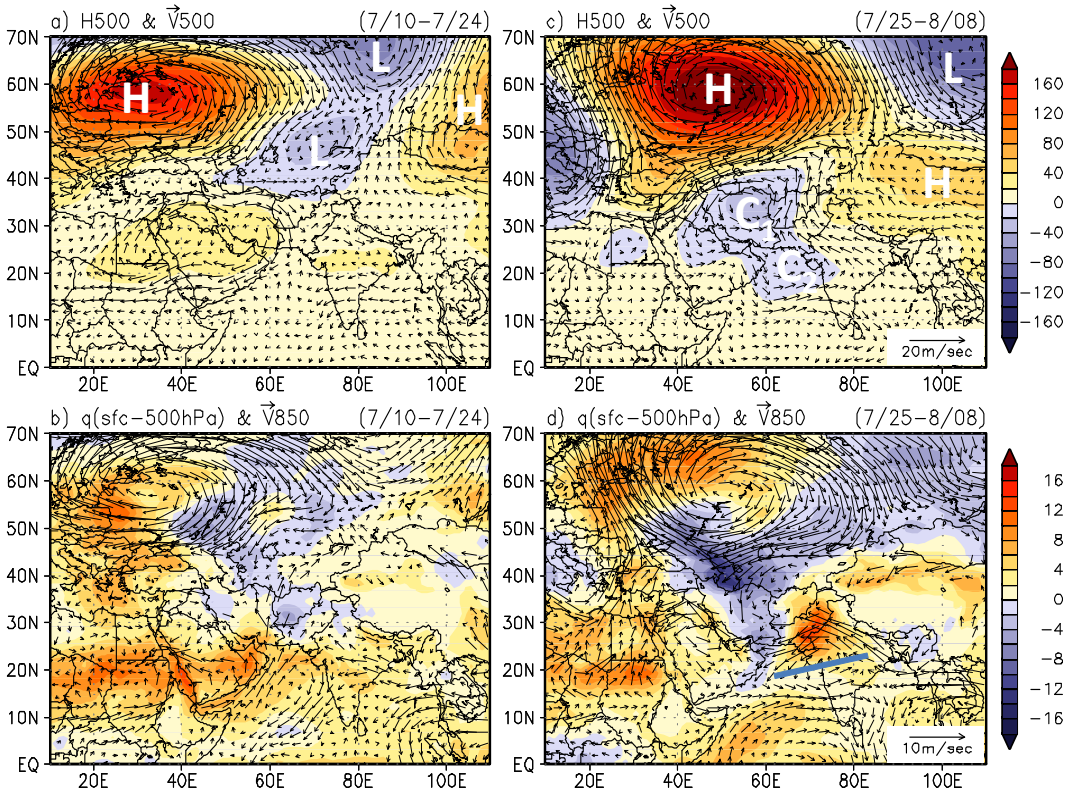

Figure 4 Spatial patterns of a) 500 hPa geopotential height (m) and wind (ms^{-1}) anomalies during Period-I, b) 850 hPa wind and precipitable water (mm) below 500hPa during Period-I, c) 500 hPa geopotential height and wind anomalies during Period-II, and d) anomalous 850 hPa wind and precipitable water during Period-II. Centers of the blocking high (H), and low (L) and the mid-tropospheric cyclones (C_1 and C_2) are marked. Thick line in Fig. 4d indicates the location of monsoon front. Anomalies were computed based on the climatology of 1979–2009.

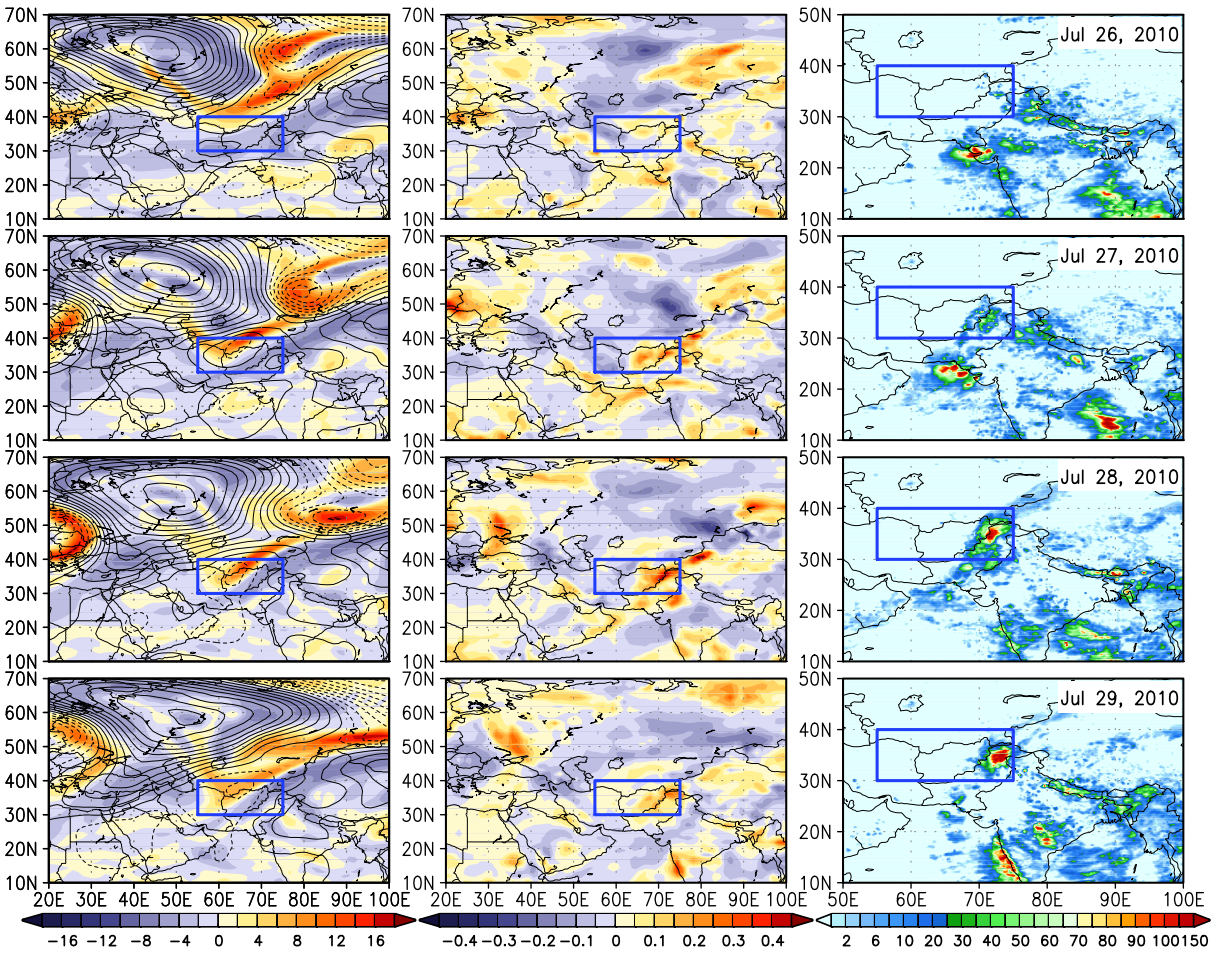

Figure 5 Daily sequence during July 26-29 of MERRA 300 hPa vorticity (10^{-5} s^{-1}) and 500 hPa height (m)anomalies (left panels), 500 hPa vertical motion (Pa s^{-1}) (middle panels), and TRMM rainfall (right panels). The target region of northern Pakistan and vicinity to the west is indicated by the rectangle. The sign of the vertical motion (middle panels) is reversed so that positive value (red) indicates ascending motion.

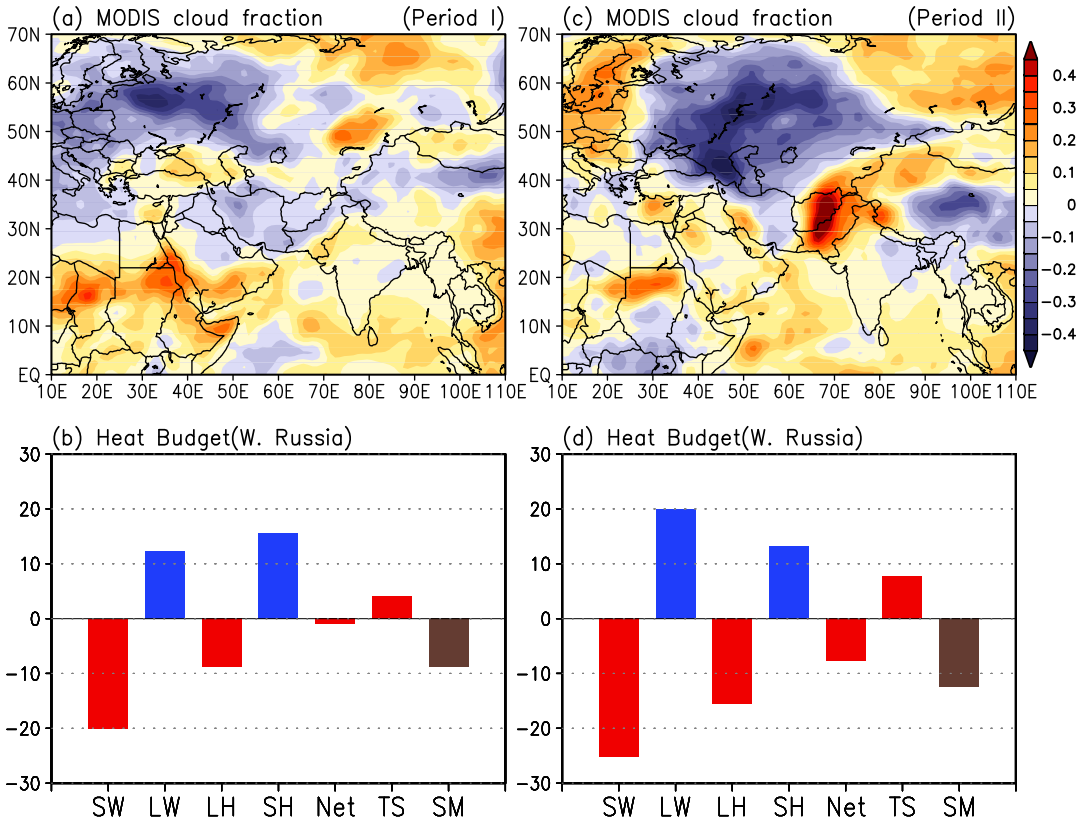

Figure 6. Upper panels: Distribution of MODIS cloud fraction anomalies for a) Period I, and c) Period II. Anomalies were computed based on the climatology of March 2000-February 2010. Lower panels: Area mean MERRA shortwave (SW) and longwave (LW) radiation, latent heat (LH) and sensible heat (SH) flux, net flux (Net) at the surface, and soil moisture (SM) averaged over western Russia [45-65^{o} N, 30-60^{o}E] for b) Period I, and d) Period II. Units are W/m^{2} for fluxes and fraction (times 100) for soil moisture. Red (blue) color denotes warming (cooling) of the land surface

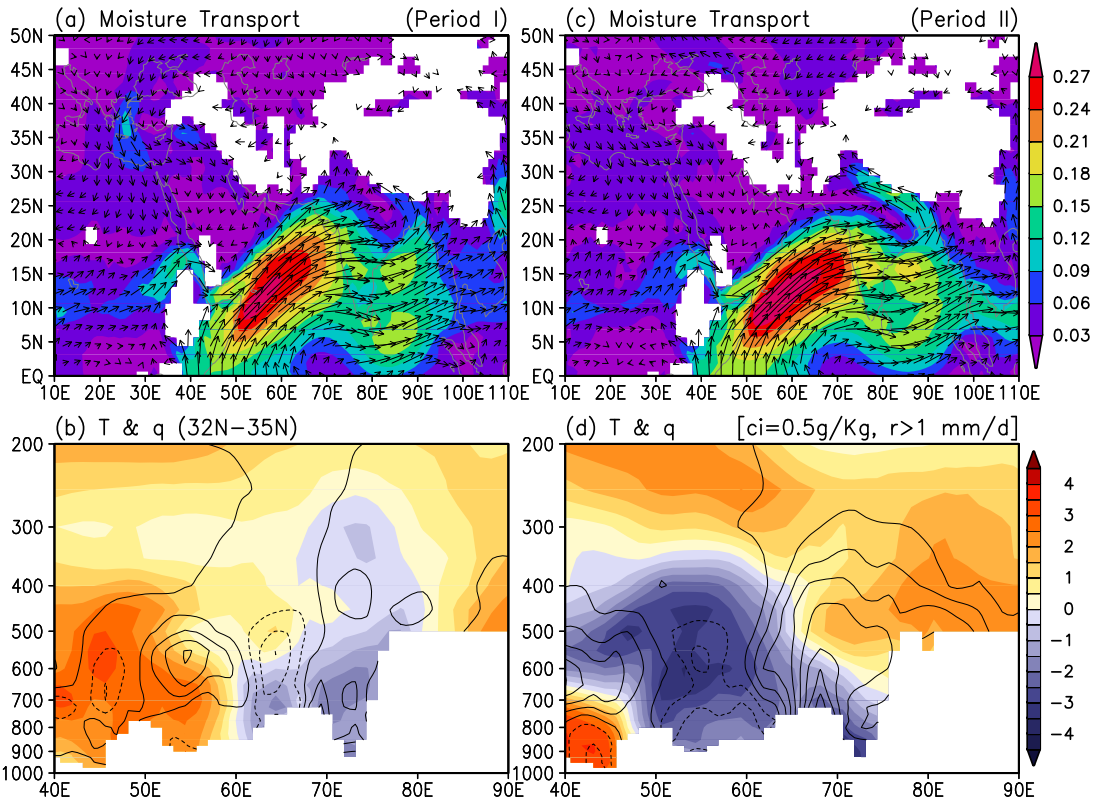

Figure 7 Upper panels: Distribution of vertically integrated moisture transport between surface to 850hPa for a) Period I, and c) Period II. Amplitude is shown in shading. Lower panels: Composite longitude-height cross-section of temperature (shading) and moisture (contour) anomalies averaged between 32 N – 35N, during rainy days (rain rate > 1 mm day^{-1}) in the northern Pakistan (See Fig. 1) for b) Period I, and d) Period II.

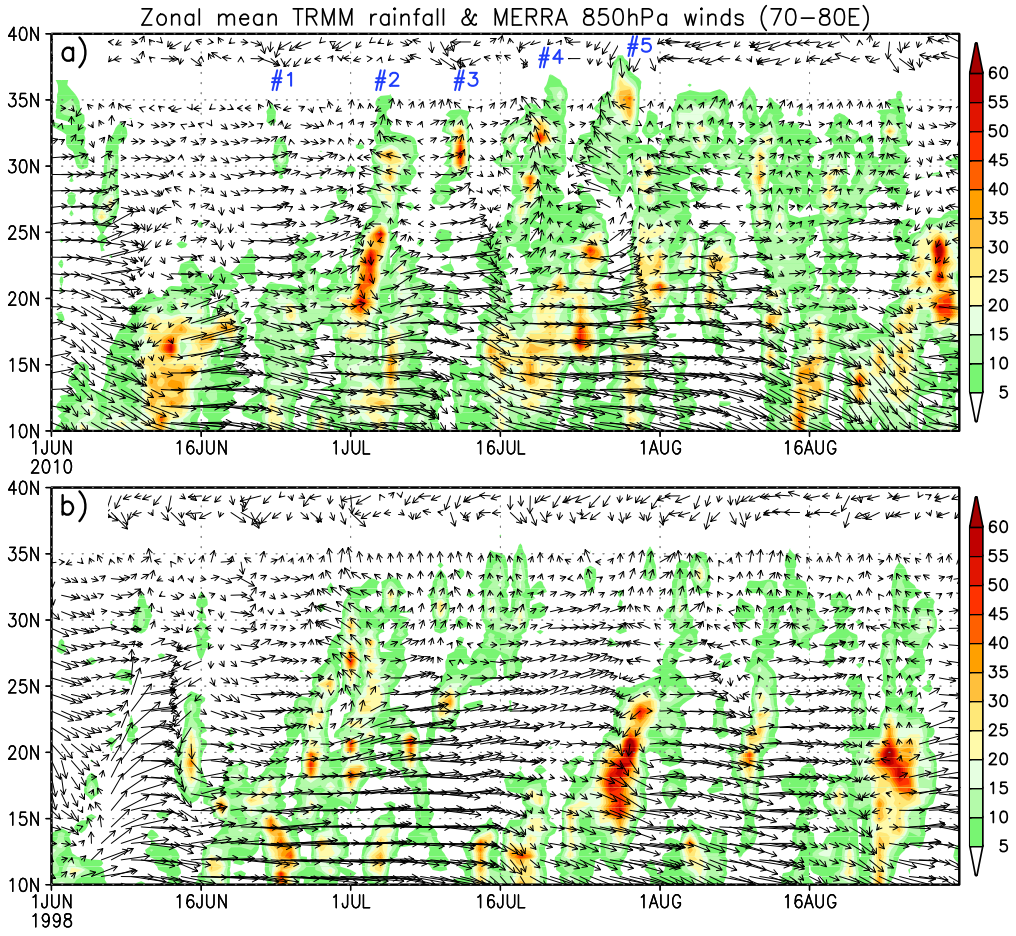

Figure 8 Latitude-time cross section of TRMM daily rainfall (mm day^{-1}) and MERRA winds at 850hPa averaged between 70^{o}E and 80^{o}E for (a) 2010 and (b) 1998.